

Channel-decomposed one-loop RG for the 2D Hubbard model¹

Christoph Husemann²
(together with M. Salmhofer,
J. Ortloff, and C. Honerkamp)

Institut für Theoretische Physik
Universität Heidelberg

Seattle, 26. February 2010

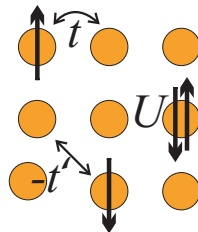
¹Phys. Rev. B 79, 195125 (2009)

²c.husemann@thphys.uni-heidelberg.de

The 2D Hubbard Model

$$\mathcal{H}[a^\dagger, a] = \sum_{\substack{\mathbf{p} \in \Gamma^* \\ \sigma = \pm}} \varepsilon(\mathbf{p}) a_{\mathbf{p}, \sigma}^\dagger a_{\mathbf{p}, \sigma} + U \sum_{x \in \Gamma} n_+(x) n_-(x)$$

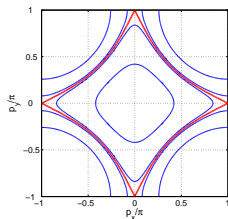
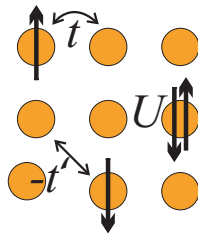
- no apparent dominant energy scale
- no apparent MF order



The 2D Hubbard Model

$$\mathcal{H}[a^\dagger, a] = \sum_{\substack{\mathbf{p} \in \Gamma^* \\ \sigma = \pm}} \varepsilon(\mathbf{p}) a_{\mathbf{p}, \sigma}^\dagger a_{\mathbf{p}, \sigma} + U \sum_{x \in \Gamma} n_+(x) n_-(x)$$

- no apparent dominant energy scale
- no apparent MF order



- high- T_c cuprates near half filling (?)

[Anderson 1987, Zhang and Rice 1988]

- van Hove filling: $\nabla \varepsilon = 0$ on Fermi surface
 - logarithmic divergence in density of states
 - may increase T_c
 - interplay FM and SC

The Functional Renormalization Group (or "exact")

Idea

[Wilson, 1973]

Integrate **all** fluctuations systematically step by step.

- 1 sort fluctuations by energy, inverse length, or temperature scale Λ
- 2 integrate fluctuations with scale $> \Lambda$
- 3 calculate the change of the vertex functions as Λ decreases
- 4 if $\Lambda \rightarrow 0$ can be taken, obtain full vertex functions of the model

The Functional Renormalization Group (or "exact")

Idea

[Wilson, 1973]

Integrate **all** fluctuations systematically step by step.

- 1 sort fluctuations by energy, inverse length, or temperature scale Λ
- 2 integrate fluctuations with scale $> \Lambda$
- 3 calculate the change of the vertex functions as Λ decreases
- 4 if $\Lambda \rightarrow 0$ can be taken, obtain full vertex functions of the model

Advantages

- manages to treat infrared (also UV) singularities
- does not depend on scaling Ansatzes
- allows to make controllable approximations [Feldman, Knörrer, Trubowitz, Balaban, Gallavotti, Salmhofer]

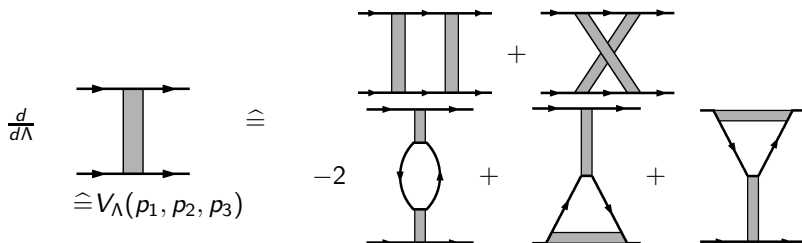
The Interaction Vertex

$$\mathcal{V}_\Lambda[\Psi] = \frac{1}{2} \int d p_1 \dots d p_3 V_\Lambda(p_1, p_2, p_3) \sum_{\substack{\sigma, \sigma' \\ \in \{+, -\}}} \bar{\psi}_\sigma(p_1) \bar{\psi}_{\sigma'}(p_2) \psi_{\sigma'}(p_3) \psi_\sigma(p_4)$$

The Interaction Vertex

$$\mathcal{V}_\Lambda[\Psi] = \frac{1}{2} \int dp_1 \dots dp_3 V_\Lambda(p_1, p_2, p_3) \sum_{\substack{\sigma, \sigma' \\ \in \{+, -\}}} \bar{\psi}_\sigma(p_1) \bar{\psi}_{\sigma'}(p_2) \psi_{\sigma'}(p_3) \psi_\sigma(p_4)$$

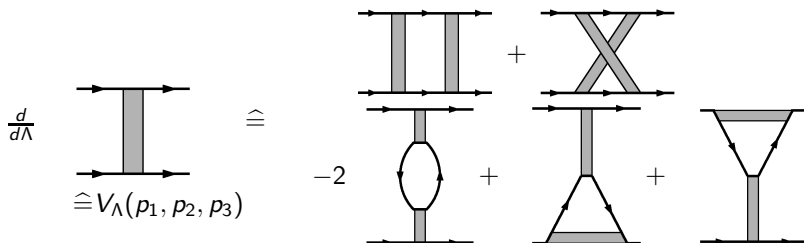
- one-loop approximation



The Interaction Vertex

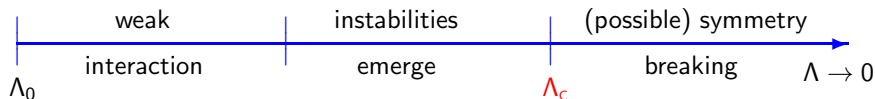
$$\mathcal{V}_\Lambda[\Psi] = \frac{1}{2} \int dp_1 \dots dp_3 V_\Lambda(p_1, p_2, p_3) \sum_{\substack{\sigma, \sigma' \\ \in \{+, -\}}} \bar{\psi}_\sigma(p_1) \bar{\psi}_{\sigma'}(p_2) \psi_{\sigma'}(p_3) \psi_\sigma(p_4)$$

- one-loop approximation



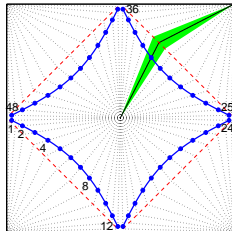
- 3 scale regimes of the RG flow

Honerkamp and Salmhofer, 2001



N -Patch Schemes

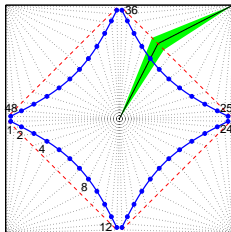
- neglect frequency dependence
- divide momentum space into N patches
- solve $\sim N^3$ ordinary differential equations



Zanchi and Schulz, 1998

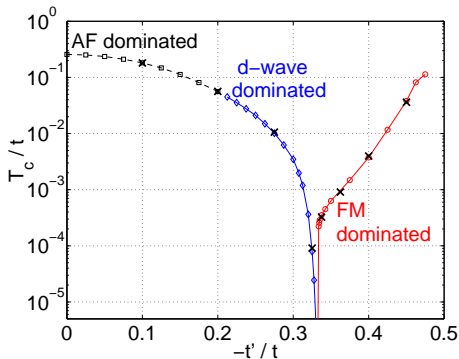
N -Patch Schemes

- neglect frequency dependence
- divide momentum space into N patches
- solve $\sim N^3$ ordinary differential equations



Zanchi and Schulz, 1998

Temperature RG Flow Honerkamp and Salmhofer, 2001



- instabilities at van Hove filling
- ferromagnetism not artificially suppressed

Parametrization of the Vertex Function

$$\frac{d}{d\Lambda} \hat{=} V(p_1, p_2, p_3) \hat{=} \begin{array}{c} \text{Diagram 1} \\ \text{Diagram 2} \\ \text{Diagram 3} \\ \text{Diagram 4} \\ \text{Diagram 5} \end{array}$$

The diagram illustrates the parametrization of the vertex function derivative. On the left, a vertical shaded bar with two horizontal arrows pointing right is labeled $\hat{=} V(p_1, p_2, p_3)$. This is followed by an equivalence symbol $\hat{=}$. To the right, a sum of five diagrams is shown, separated by plus signs. The first diagram is a vertical shaded bar with two horizontal arrows pointing right. The second diagram is a vertical shaded bar with two horizontal arrows pointing right, and a shaded oval with two arrows forming a loop on top. The third diagram is a vertical shaded bar with two horizontal arrows pointing right, and a shaded triangle with two arrows pointing down on top. The fourth diagram is a vertical shaded bar with two horizontal arrows pointing right, and a shaded X-shape with two arrows pointing down on top. The fifth diagram is a vertical shaded bar with two horizontal arrows pointing right, and a shaded inverted triangle with two arrows pointing up on top. A coefficient of -2 is placed to the left of the second diagram.

Observation: The leading weak coupling instabilities are mainly determined by the *singular* momentum and frequency structure of the flow equation.

Definition of 3 Channels

$$\begin{aligned}
 \dot{\Phi}_{\text{SC}}^{\Lambda}(p_1, p_3, p_1 + p_2) &\hat{=} - \text{[Diagram: Two vertical shaded bars, each with two horizontal lines passing through them. The top two lines have arrows pointing right. The bottom two lines have arrows pointing left.]}, \quad \dot{\Phi}_{\text{M}}^{\Lambda}(p_1, p_2, p_3 - p_1) \hat{=} \text{[Diagram: Two crossed shaded bars, each with two horizontal lines passing through them. The top two lines have arrows pointing right. The bottom two lines have arrows pointing left.]} \\
 \dot{\Phi}_{\text{K}}^{\Lambda}(p_1, p_2, p_2 - p_3) &\hat{=} 4 \text{[Diagram: A vertical shaded bar with two horizontal lines passing through it. The top line has an arrow pointing right, the bottom line has an arrow pointing left. A shaded oval is drawn around the bar between the two lines.]} - 2 \text{[Diagram: A shaded triangle with a vertical shaded bar on its top edge. The top horizontal line has an arrow pointing right. The two slanted lines have arrows pointing down towards the bar.]} - 2 \text{[Diagram: A shaded inverted triangle with a vertical shaded bar on its bottom edge. The bottom horizontal line has an arrow pointing right. The two slanted lines have arrows pointing down towards the bar.]} + \text{[Diagram: Two crossed shaded bars, each with two horizontal lines passing through them. The top two lines have arrows pointing right. The bottom two lines have arrows pointing left. A vertical double-headed arrow is to the right of the diagram.]}
 \end{aligned}$$

mit $\Phi_{\text{SC}}^{\Lambda_0} = \Phi_{\text{M}}^{\Lambda_0} = \Phi_{\text{K}}^{\Lambda_0} = 0$

Definition of 3 Channels

$$\begin{aligned}
 \dot{\Phi}_{\text{SC}}^{\Lambda}(p_1, p_3, p_1 + p_2) &\hat{=} - \text{[Diagram: Two vertical shaded bars with horizontal arrows above and below them]} \\
 \dot{\Phi}_{\text{K}}^{\Lambda}(p_1, p_2, p_2 - p_3) &\hat{=} 4 \text{ [Diagram: A vertical shaded bar with a loop on top]} - 2 \text{ [Diagram: A triangle with shaded top and bottom edges]} - 2 \text{ [Diagram: An inverted triangle with shaded top and bottom edges]} + \text{[Diagram: Two crossed shaded bars with horizontal arrows above and below them]} \\
 \dot{\Phi}_{\text{M}}^{\Lambda}(p_1, p_2, p_3 - p_1) &\hat{=} \text{[Diagram: Two crossed shaded bars with horizontal arrows above and below them]}
 \end{aligned}$$

mit $\Phi_{\text{SC}}^{\Lambda_0} = \Phi_{\text{M}}^{\Lambda_0} = \Phi_{\text{K}}^{\Lambda_0} = 0$

The vertex function

$$\begin{aligned}
 V(p_1, p_2, p_3) &= U - \Phi_{\text{SC}}^{\Lambda}(p_1, p_3, p_1 + p_2) + \Phi_{\text{M}}^{\Lambda}(p_1, p_2, p_3 - p_1) \\
 &\quad + \frac{1}{2} \Phi_{\text{M}}^{\Lambda}(p_1, p_2, p_2 - p_3) - \frac{1}{2} \Phi_{\text{K}}^{\Lambda}(p_1, p_2, p_2 - p_3)
 \end{aligned}$$

The Effective Two-Fermion Interaction

$$\mathcal{V}_\Lambda[\Psi] = \mathcal{V}_{\text{H.M.}}[\Psi] + \mathcal{V}_{\text{SC}}^\Lambda[\Psi] + \mathcal{V}_{\text{M}}^\Lambda[\Psi] + \mathcal{V}_{\text{K}}^\Lambda[\Psi]$$

$$\mathcal{V}_{\text{SC}}^\Lambda[\Psi] = -\frac{1}{4} \int dq dq' dl \Phi_{\text{SC}}^\Lambda(q, q', l) \sum_{J=0}^3 \left(\bar{\Psi}(q) \sigma^{(J)} \bar{\Psi}(l - q) \right) \left(\Psi(q') \sigma^{(J)} \Psi(l - q') \right)$$

"superconductivity"

The Effective Two-Fermion Interaction

$$\mathcal{V}_\Lambda[\Psi] = \mathcal{V}_{\text{H.M.}}[\Psi] + \mathcal{V}_{\text{SC}}^\Lambda[\Psi] + \mathcal{V}_{\text{M}}^\Lambda[\Psi] + \mathcal{V}_{\text{K}}^\Lambda[\Psi]$$

$$\mathcal{V}_{\text{SC}}^\Lambda[\Psi] = -\frac{1}{4} \int dq dq' dl \Phi_{\text{SC}}^\Lambda(q, q', l) \sum_{J=0}^3 \left(\bar{\Psi}(q) \sigma^{(J)} \bar{\Psi}(l - q) \right) \left(\Psi(q') \sigma^{(J)} \Psi(l - q') \right)$$

"superconductivity"

$$\mathcal{V}_{\text{M}}^\Lambda[\Psi] = -\frac{1}{4} \int dq dq' dl \Phi_{\text{M}}^\Lambda(q, q', l) \sum_{j=1}^3 \left(\bar{\Psi}(q) \sigma^{(j)} \Psi(q + l) \right) \left(\bar{\Psi}(q') \sigma^{(j)} \Psi(q' - l) \right)$$

"magnetism"

$$\mathcal{V}_{\text{K}}^\Lambda[\Psi] = -\frac{1}{4} \int dq dq' dl \Phi_{\text{K}}^\Lambda(q, q', l) \left(\bar{\Psi}(q) \Psi(q + l) \right) \left(\bar{\Psi}(q') \Psi(q' - l) \right)$$

"forward scattering"

Decomposition of the Superconducting Channel

$$\Phi_{\text{SC}}^{\Lambda}(q, q', l) = \sum_{mn} D_{mn}(l) f_m(\frac{1}{2} - \mathbf{q}) f_n(\frac{1}{2} - \mathbf{q}') + R_{\text{SC}}(q, q', l)$$

$$\hat{=} \sum_{mn} \text{Diagram} + R_{\text{SC}}(q, q', l)$$

The diagram shows two circles, labeled 'm' and 'n', connected by a wavy line. Each circle has two external lines with arrows pointing outwards, representing fermion legs.

Decomposition of the Superconducting Channel

$$\Phi_{\text{SC}}^{\Lambda}(q, q', l) = \sum_{mn} D_{mn}(l) f_m(\frac{1}{2} - \mathbf{q}) f_n(\frac{1}{2} - \mathbf{q}') + R_{\text{SC}}(q, q', l)$$

$$\cong \sum_{mn} \text{Diagram} + R_{\text{SC}}(q, q', l)$$


The diagram shows two circles labeled 'm' and 'n' connected by a wavy line. Each circle has two external arrows pointing outwards, representing fermion lines.

that is,

$$\mathcal{V}_{\text{SC}}^{\Lambda}[\Psi] = -\frac{1}{4} \sum_{mn} \int dl D_{mn}(l) \sum_{J=0}^3 \int dq \left(\bar{\Psi}(q) \sigma^{(J)} \bar{\Psi}(l - q) \right) f_m(\frac{1}{2} - q)$$

$$\int dq' \left(\Psi(q') \sigma^{(J)} \Psi(l - q') \right) f_n(\frac{1}{2} - q') + \mathcal{R}_{\text{SC}}[\Psi]$$

Decomposition of the Superconducting Channel

$$\begin{aligned}\Phi_{\text{SC}}^{\Lambda}(q, q', l) &= \sum_{mn} D_{mn}(l) f_m\left(\frac{1}{2} - \mathbf{q}\right) f_n\left(\frac{1}{2} - \mathbf{q}'\right) + R_{\text{SC}}(q, q', l) \\ &\hat{=} \sum_{mn} \text{Diagram} + R_{\text{SC}}(q, q', l)\end{aligned}$$


For a *curved* and *regular* Fermi surface

- particle–hole graphs are marginal
- the most attractive eigenvalue of $D(0)$ determines symmetry of the gap
- particle–hole graphs induce attractive eigenvalues of $D(0)$

Magnetic and Forward Scattering Channel

$$\Phi_M^\Lambda(q, q', l) = \sum_{mn} M_{mn}(l) f_m(\mathbf{q} + \frac{1}{2}) f_n(\mathbf{q}' - \frac{1}{2}) + R_M(q, q', l)$$

$$\cong \sum_{mn} \begin{array}{c} \nearrow \\ \boxed{m} \\ \searrow \end{array} \text{---} \begin{array}{c} \nwarrow \\ \boxed{n} \\ \swarrow \end{array} + R_M(q, q', l)$$

$$\Phi_K^\Lambda(q, q', l) = \sum_{mn} K_{mn}(l) f_m(\mathbf{q} + \frac{1}{2}) f_n(\mathbf{q}' - \frac{1}{2}) + R_K(q, q', l)$$

$$\cong \sum_{mn} \begin{array}{c} \nwarrow \\ \boxed{m} \\ \swarrow \end{array} \text{---} \begin{array}{c} \swarrow \\ \boxed{n} \\ \nwarrow \end{array} + R_K(q, q', l)$$

Channel Decomposition: Summary

$$\begin{aligned}
 &= U + \sum_{m,n} \left\{ - \text{circle}(m) \overset{D}{\text{wavy}} \text{circle}(n) + \text{triangle}(m) \overset{M}{\text{solid}} \text{triangle}(n) \right. \\
 &\quad \left. + \frac{1}{2} \text{triangle}(m) \overset{M}{\text{solid}} \text{triangle}(n) - \frac{1}{2} \text{square}(m) \overset{K}{\text{solid}} \text{square}(n) \right\} + \mathcal{R}
 \end{aligned}$$

bilinears:

$$\begin{aligned}
 \text{circle}(n) &= \int dq \bar{\Psi}(q) \sigma^{(j)} \bar{\Psi}(l-q) f_n\left(\frac{l}{2} - q\right) \\
 \text{triangle}(n) &= \int dq \bar{\Psi}(q) \sigma^{(j)} \Psi(q+l) f_n\left(q + \frac{l}{2}\right) \\
 \text{square}(n) &= \int dq \bar{\Psi}(q) \Psi(q+l) f_n\left(q + \frac{l}{2}\right)
 \end{aligned}$$

Channel Decomposition: Summary

$$\begin{aligned}
 &= \mathbf{U} + \sum_{m,n} \left\{ - \text{diagram with wavy line } D + \text{diagram with straight line } M \right. \\
 &\quad \left. + \frac{1}{2} \text{diagram with straight line } M - \frac{1}{2} \text{diagram with straight line } K \right\} + \mathcal{R}
 \end{aligned}$$

Remainder term \mathcal{R}

- under control for curved and regular Fermi surfaces
- in general: choose f 's such that they are "small"

... is dropped at first.

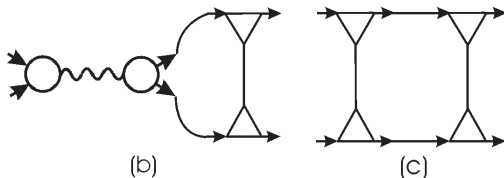
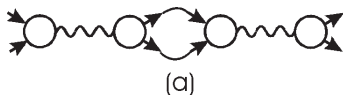
The Boson Propagator Flow

$$\begin{array}{c} \text{---} \circ \text{---} \\ \text{---} \end{array} \begin{array}{c} \bullet \\ \text{---} \end{array} \begin{array}{c} \circ \text{---} \\ \text{---} \end{array} = P_{mn}^{\text{SC}} \left[\begin{array}{c} \text{---} \circ \text{---} \\ \text{---} \end{array} \begin{array}{c} \bullet \\ \text{---} \end{array} \begin{array}{c} \circ \text{---} \\ \text{---} \end{array} - \text{---} \text{---} \text{---} - \frac{3}{2} \begin{array}{c} \text{---} \text{---} \\ \text{---} \end{array} + \frac{1}{2} \begin{array}{c} \text{---} \text{---} \\ \text{---} \end{array} \right]^2$$

The Boson Propagator Flow

$$\begin{array}{c} \circlearrowleft \\ \circlearrowright \end{array} \begin{array}{c} \bullet \\ \circlearrowleft \\ \circlearrowright \end{array} \begin{array}{c} \circlearrowleft \\ \circlearrowright \end{array} = P_{mn}^{SC} \left[\begin{array}{c} \circlearrowleft \\ \circlearrowright \end{array} \begin{array}{c} \bullet \\ \circlearrowleft \\ \circlearrowright \end{array} \begin{array}{c} \circlearrowleft \\ \circlearrowright \end{array} - \begin{array}{c} \text{---} \\ \text{---} \\ \text{---} \end{array} - \frac{3}{2} \begin{array}{c} \text{---} \\ \text{---} \\ \text{---} \end{array} + \frac{1}{2} \begin{array}{c} \text{---} \\ \text{---} \\ \text{---} \end{array} \right]^2$$

three examples, how the square is taken:



The Boson Propagator Flow

$$\text{Diagram 1} = P_{mn}^{\text{SC}} \left[\text{Diagram 2} - \text{Diagram 3} - \frac{3}{2} \text{Diagram 4} + \frac{1}{2} \text{Diagram 5} \right]^2$$

Diagram 1: A wavy boson line with vertices m and n .

Diagram 2: A circle boson line with vertices m and n .

Diagram 3: A horizontal fermion line with two vertices.

Diagram 4: A vertical fermion line with two vertices.

Diagram 5: A square fermion loop with two vertices.

$$\text{Diagram 6} = -P_{mn}^{\text{M}} \left[\text{Diagram 7} + \text{Diagram 3} - \text{Diagram 8} + \frac{1}{2} \text{Diagram 4} - \frac{1}{2} \text{Diagram 5} \right]^2$$

Diagram 6: A fermion line with vertices m and n .

Diagram 7: A triangle fermion loop with vertices m and n .

Diagram 8: A vertical boson line with two vertices.

$$\text{Diagram 9} = -P_{mn}^{\text{K}} \left[\text{Diagram 10} - \text{Diagram 3} + \text{Diagram 8} - \frac{3}{2} \text{Diagram 4} - \frac{1}{2} \text{Diagram 5} \right]^2$$

Diagram 9: A fermion line with vertices m and n .

Diagram 10: A square fermion loop with vertices m and n .

Specific Set-up of the RG Flow

- RG scale $\Lambda = \Omega$ is decreased in the flow

$$\frac{1}{ip_0 - \varepsilon(\mathbf{p}) + \mu} \frac{p_0^2}{p_0^2 + \Omega^2}$$

- treat scales $\Omega > \Omega_0$ by perturbation theory in $\frac{U}{\Omega_0}$

Specific Set-up of the RG Flow

- RG scale $\Lambda = \Omega$ is decreased in the flow

$$\frac{1}{ip_0 - \varepsilon(\mathbf{p}) + \mu} \frac{p_0^2}{p_0^2 + \Omega^2}$$

- treat scales $\Omega > \Omega_0$ by perturbation theory in $\frac{U}{\Omega_0}$

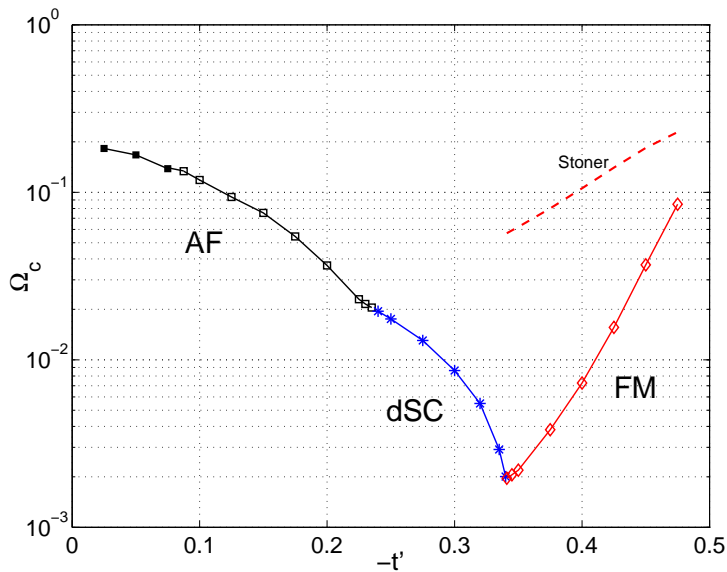
- form factors: only

$$f_1(\mathbf{p}) = 1 \quad (s\text{-wave})$$

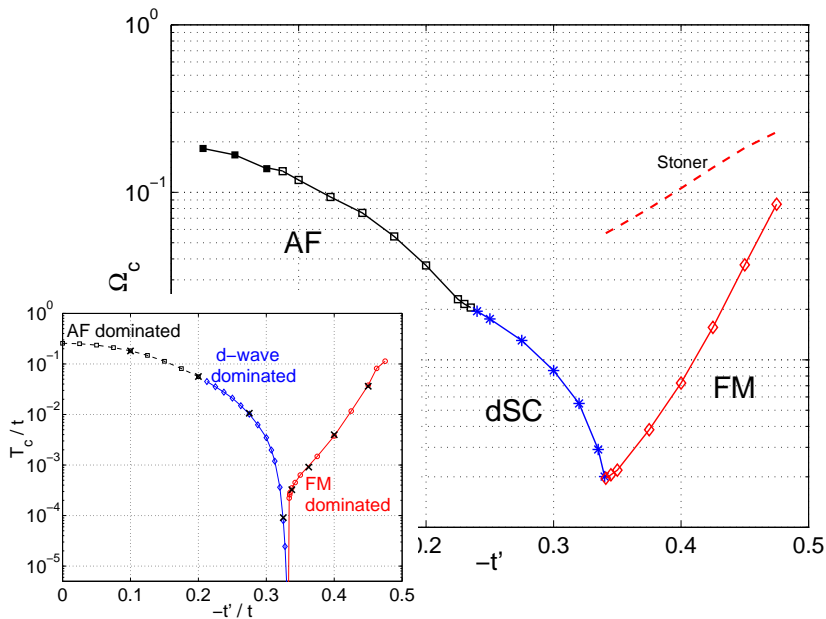
$$f_2(\mathbf{p}) = \cos p_x - \cos p_y \quad (d_{x^2-y^2}\text{-wave})$$

- boson propagators:
 - neglect frequency dependence
 - approximate momentum dependence numerically [step functions with high accuracy for transfer momenta $\approx (0, 0), (\pi, \pi)$]

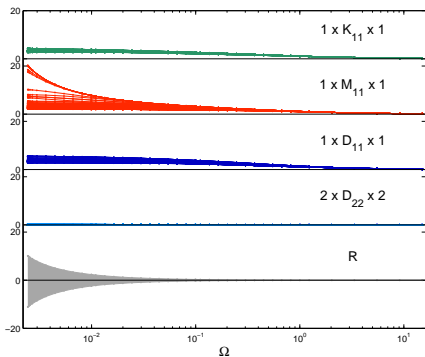
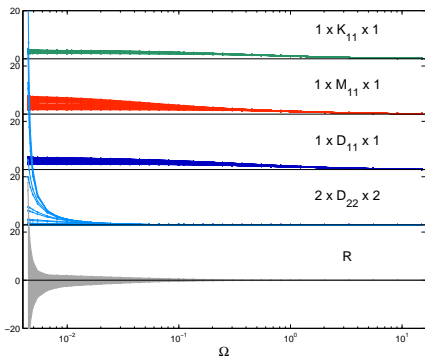
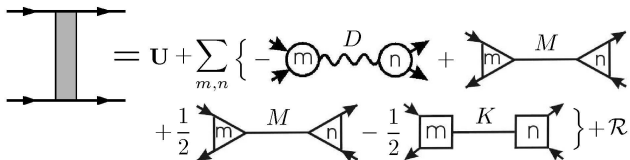
Instabilities at Van Hove Filling, $U = 3t$, and $T = 0$



Instabilities at Van Hove Filling, $U = 3t$, and $T = 0$



Remainder Estimation J. Ortloff, C.H., C. Honerkamp, M. Salmhofer



And Now?

The proposed parametrization of the vertex function

- allows to identify leading instabilities,
- shows that the vertex function is singular only at points, and
- allows Hubbard–Stratonovich transformations.



Ω_0

Ω_c

And Now?

The proposed parametrization of the vertex function

- allows to identify leading instabilities,
- shows that the vertex function is singular only at points, and
- allows Hubbard–Stratonovich transformations.

Continuation of the RG flow into an ordered phase

- **fermions** Salmhofer et al.
- **bosons** Metzner et al.
- **fermions and bosons** Wetterich et al., Metzner et al., Kopietz et al.

Ω_0

Ω_c

Effective Model at Scale Ω_c

eg. keep only $d_{x^2-y^2}$ -wave superconductivity

$$Z = \int \mathcal{D}[\Psi] \exp \left\{ -\frac{1}{2}(\Psi, G_{\Omega_c}^{-1} \Psi) - (\bar{X}, D_{11} X) \right\}$$

with

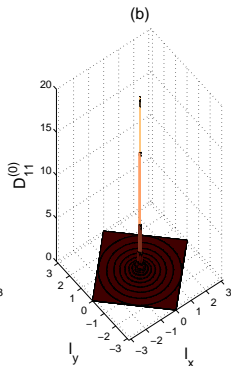
$$\bar{X}(l) = \frac{1}{2} \int dq \bar{\Psi}(q) \epsilon \bar{\Psi}(l-q) f_1\left(\frac{l}{2} - q\right)$$

Effective Model at Scale Ω_c

eg. keep only $d_{x^2-y^2}$ -wave superconductivity

$$Z = \int \mathcal{D}[\Psi] \exp \left\{ -\frac{1}{2}(\Psi, G_{\Omega_c}^{-1} \Psi) - (\bar{X}, D_{11} X) \right\}$$

with



$$\bar{X}(l) = \frac{1}{2} \int dq \bar{\Psi}(q) \epsilon \bar{\Psi}(l-q) f_1\left(\frac{l}{2} - q\right)$$

$$G_{\Omega_c}(p) = \frac{1}{ip_0 - \epsilon(\mathbf{p}) + \mu} \frac{\Omega_c^2}{p_0^2 + \Omega_c^2}$$

↑
suppresses all fermions
that have already been
integrated out

Conclusion and Outlook

The proposed decomposition

- preserves the essential structure of the one-loop RG,
- reduces computing cost, $O(N^3) \rightarrow O(N)$ ODEs,
- reveals point-like singularities of the interaction vertex, and
- gives effective vertices near Ω_c that can be directly transformed into an effective theory of order parameter fields.

Conclusion and Outlook

The proposed decomposition

- preserves the essential structure of the one-loop RG,
- reduces computing cost, $O(N^3) \rightarrow O(N)$ ODEs,
- reveals point-like singularities of the interaction vertex, and
- gives effective vertices near Ω_c that can be directly transformed into an effective theory of order parameter fields.

Work in progress:

- adaptive flow of Ω -dependent form factors
- frequency dependence of the boson propagators
- $\Omega < \Omega_c$: competition of superconductivity and ferromagnetism?
pseudo-gap phase?